Hong–Ou–Mandel Dip Using Degenerate Photon Pairs from a Single Periodically Poled Lithium Niobate Waveguide with Integrated Mode Demultiplexer

Qiang Zhang[1*], Hiroki Takesue[2], Carsten Langrock, Xiuping Xie, Martin M. Fejer, and Yoshihisa Yamamoto[1]

Edward L. Ginzton Laboratory, Stanford University, Stanford, CA 94305, U.S.A.
[1]*National Institute of Informatics, 2-1-2 Hitotsubashi, Chiyoda, Tokyo 101-8430, Japan*
[2]*NTT Basic Research Laboratories, NTT Corporation, 3-1 Morinosato Wakamiya, Atsugi, Kanagawa 243-0198, Japan*

Received September 11, 2009; accepted March 26, 2010; published online June 21, 2010

We experimentally observed a Hong–Ou–Mandle dip with photon pairs generated in a periodically poled reverse-proton-exchange lithium niobate waveguide with an integrated mode demultiplexer at a wavelength of 1.5 μm. The visibility of the dip in the experiment was 80% without subtraction of any noise terms at a peak pump power of 4.4 mW. The technology developed in the experiment can find various applications in the research field of linear optics quantum computation in fiber or quantum optical coherence tomography with near infrared photon pairs.

DOI: 10.1143/JJAP.49.064401

1. Introduction

When two identical photons overlap at the two inputs of a beam splitter, the two photons will bunch together upon either beam splitter output and no coincidence of the two outputs will be observed. This is the so-called Hong–Ou–Mandle (HOM) dip.[1)] It was first used for precisely measuring the time duration of wide-spectral-bandwidth single photons, which were too faint to be measured using an autocorrelator. Classical light fields also exhibit a similar destructive interference, but only with a 50% visibility.[2)] Therefore, the HOM dip is often utilized to demonstrate the difference between the regime of quantum optics and its classical counterpart. Very recently, the effect found several important applications in the field of quantum information, for example, quantum teleportation,[3)] quantum repeater,[4)] linear optics quantum computation (LOQC),[5)] and quantum optical coherence tomography (QOCT),[6)] among others.

The HOM dip was first observed using visible-light photon pairs generated in a nonlinear crystal via parametric down-conversion (PDC).[1)] Soon afterwards, it was also realized using telecom-band photon pairs, either generated via PDC,[7)] or via four-wave mixing (FWM) in dispersion-shifted fiber (DSF).[8)] Also, the triggered HOM dip with independent telecom-band photons has been observed using photon pairs via PDC from a periodically poled lithium niobate (PPLN) waveguide,[9)] and via FWM in DSF[10)] or in photonic crystal fibers.[11)]

As mentioned earlier, conventional PDC is most often implemented using bulk nonlinear crystals. Recently, PPLN waveguides have been used to generate correlated photon pairs due to their higher conversion efficiency compared to their bulk counterparts.[12)] Furthermore, waveguide devices can be fiber pigtailed to achieve high coupling efficiencies, as well as simple and mechanically stable operation. However, the HOM dip has not yet been observed using degenerate photon pairs from PPLN waveguides due to the difficulty of spatially separating degenerate photon pairs. In the fiber-optic implementation, somewhat complicated methods to separate the identical photon pairs have been considered.[13)] The authors of ref. 13[13)] utilized two pump pulse trains with different wavelengths, liquid nitrogen as the cryogen to reduce the dark counts, and a quantum interferometer to separate the generated degenerate photon pairs.

In this letter, we used an asymmetric Y-junction-based mode demultiplexer realized in a reverse-proton-exchange (RPE) PPLN waveguide[14,15)] to separate the degenerate photon pairs generated in the quasi phasematching (QPM) grating in the classical regime. Now we utilized them in the quantum regime. The photon pairs were then launched into a fiber-based beam splitter and a HOM dip with a 80% visibility was observed with an average of 0.03 photon pairs per pulse without subtraction of any accidental coincidences. Such a device only uses a single integrated waveguide device to generate and separate the degenerate photon pairs, one pump pulse train, and does not require cryogenic cooling.

2. System

PDC processes in nonlinear crystals usually utilize angular or polarization-state differences between the signal and the idler photon to enable spatial separability. However, protonated z-cut Lithium Niobate waveguides only support transverse magnetic (TM) polarized waves, eliminating the possibility of polarization-based de-multiplexing. Naturally, angular de-multiplexing is impossible in a channel waveguide configuration.

Mode de-multiplexing using asymmetric Y-junctions, based on the adiabatic variation of the refractive index distribution along the device, can be utilized to solve this problem.[14,15)] Both the input and output sides have two arms, one narrow and one wide, as shown in the inset of Fig. 1. The pump wave in the TM_{00} mode is coupled into the narrow input arm of the Y-junction and is adiabatically converted into the TM_{10} mode of the main waveguide. The pump then traverses the QPM grating and generates photon pairs in different spatial modes (signal in TM_{10} and idler in TM_{00}, respectively). The idler photon in the TM_{00} mode will exit via the wide arm of the Y-junction's output port, while the signal photon in the TM_{10} mode will be coupled into the narrow arm. Both output modes are then adiabatically transformed to TM_{00} modes with identical sizes. For wavelengths near 1.5 μm, an extinction ratio of ~30 dB between the two output modes can be achieved with current fabrication technologies.[14,15)]

In the experiment, an external-cavity diode laser operating at a wavelength of 1559 nm was modulated by an optical

*E-mail address: qiangzh@stanford.edu

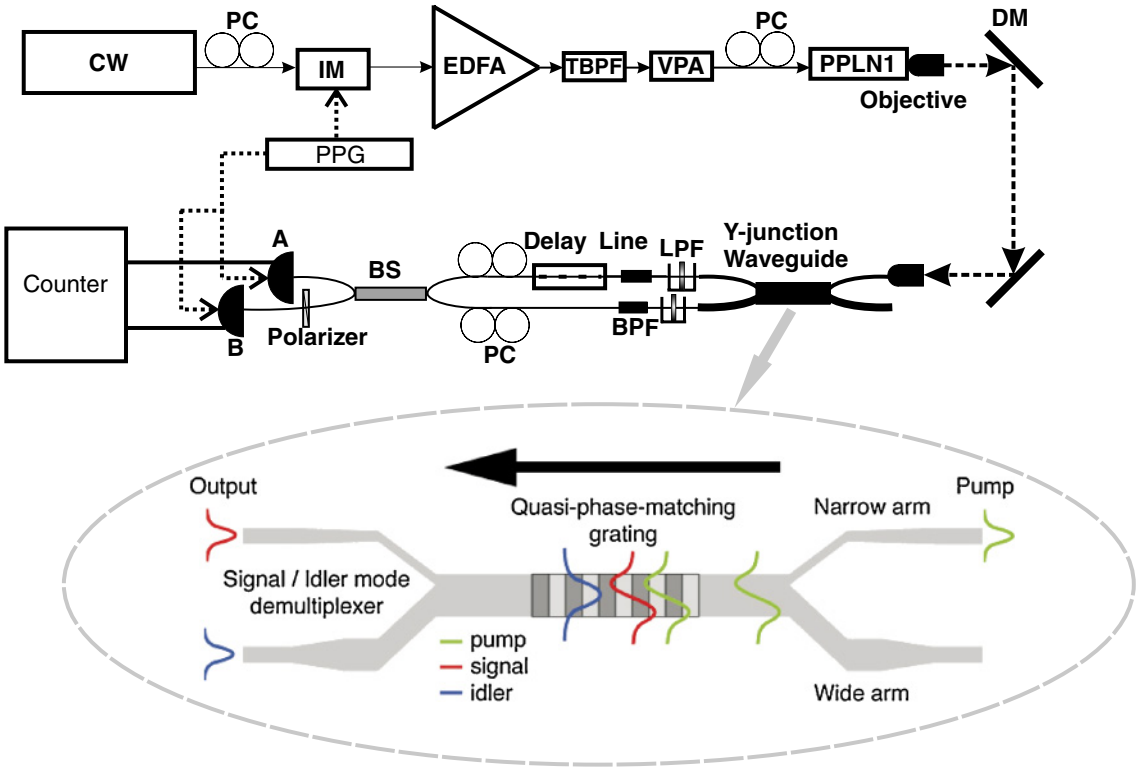

Fig. 1. (Color online) Diagram of the experimental setup; IM: intensity modulator, VPA: variable power attenuator, A and B: InGaAs APDs, BS: beam splitter. The inset is the structure of the asymmetric Y-junction containing PPLN waveguide.

intensity modulator into pulse trains with 100-MHz repetition rate and 90-ps pulse width. As shown in Fig. 1, the 100-MHz signal for the amplitude modulator was derived from a pulse-pattern-generator (PPG). After being amplified by an erbium-doped fiber amplifier (EDFA), the laser pulses with an average power of 11.48 mW passed through a 3-nm-wide tunable bandpass filter (TBPF) to reduce the spontaneous emission noise from the EDFA. A variable attenuator was inserted after the bandpass filter to regulate the pump power. The pump was then frequency doubled in using a PPLN waveguide chip (PPLN1). Since these waveguide devices only accept TM-polarized light, an in-line polarization controller (PC) was used to adjust the polarization before the device. The residual pump exiting the PPLN1 was attenuated by 180 dB using dichroic mirrors (DM). The second harmonic (SH) wave was then launched into the second asymmetric-Y-junction-containing PPLN waveguide to serve as the pump for the PDC process. The two output ports were fiber pigtailed to improve the collection efficiency and stability of operation. A fiber U-bench (Thorlabs FB220-FC) with several long-pass filters (LPF) was inserted into each output fiber of the second PPLN chip to eliminate residual SH and other nonlinear fluorescence components. The second PPLN waveguide was operated at degeneracy by adjusting the crystal temperature. The bandwidth of the down-converted photon pairs was 40 nm, such that the group velocity dispersion in the PPLN waveguide could not be ignored. Two 0.8-nm-wide BPFs were used to reduce the spectral width and define the photon pairs' coherence time as 4 ps (FWHM).

The photon pairs were combined at a 50 : 50 fiber-based beam splitter. To achieve perfect temporal overlap, the signal photons passed through a variable fiber-coupled free-space delay line before being launched into the beam splitter. The minimum step size of the delay line was about 30 fs, which was much smaller than the photon pairs' coherence time of 4 ps. Since the fiber-based components used in this experiment were not polarization maintaining, we inserted a polarization controller into each channel and one polarizer before detector B to equalize the polarization of the two photons.

We used two InGaAs avalanche photodiodes (APDs) operated in the gated mode with a 5-MHz gate frequency and 1-ns time window to detect the output photons of the beam splitter. The gate pulses were synchronized to the incoming photons using the PPG. The quantum efficiency and dark-count rates per time window of the detectors were 10% (both), 5×10^{-7} and 1.6×10^{-6} Hz, respectively. The two detectors were connected to a counter for coincidence measurements.

3. Theory and Results

When the pump-pulse duration is longer than the photon-pair coherence time in the PDC process, which was the case in our experiment, the pair generation probability obeys Poissionian statistics,[16–18] i.e.,

$$P_n = \frac{\mu^n}{n!}\exp(-\mu), \tag{1}$$

where P_n is the probability of generation of n pairs of correlated photons, and μ is the average photon-pair number per pulse.

The parameter μ is very important for analyzing the visibility of the HOM dip and can be estimated by looking at

the coincidence accidental ratio (CAR).[19] To measure the CAR, we slightly modified the experimental setup shown in Fig. 1 as follows. We exchanged the counter for a time interval analyzer (TIA) and purposely misaligned the fiber delay's position away from the HOM dip condition. The detection events of the signal and idler channels were used as start and stop signals of the TIA, respectively. A coincidence in the matched time slot represents the true coincidence caused by photons generated with the same pump pulse, while a coincidence in the unmatched time slot represents the accidental coincidence mainly caused by photons generated by different pump pulses. The ratio between the two coincidence rates is the CAR. In our experiment, the CAR reached 29.4 at a peak pump power of 4.4 mW, corresponding to a μ of 0.03 per pulse.

Since the spectral shape of the 0.8-nm-wide BPFs was Gaussian, the shape of the photon pairs was also approximated by a Gaussian. In this case, the coincidence rate N of the HOM dip can be fitted by the following function,[7,10]

$$N = C\left[1 - \frac{2VRT}{R^2 + T^2}\exp\left(-\frac{\delta\tau^2}{2\sigma^2}\right)\right], \tag{2}$$

where $C, V, T, R, \delta\tau, \sigma$ represent the coincidence rates away from the HOM dip, visibility, the transmittance and the reflectance of the 50 : 50 coupler, the delay time, and the $1/e$ temporal half-width of the photon field. In our case, T and R were -3.3 and -3.6 dB, respectively. σ was 1.7 ps according to the 4-ps FWHM of the photon pair duration. The visibility can be expressed by[18]

$$V = 1 - \frac{\mu^2\eta^2 + 2\mu\eta D + D^2}{\mu\eta^2/2 + \mu^2\eta^2 + 2\mu\eta D + D^2}, \tag{3}$$

where η and D are the channel loss (including the detector's quantum efficiency), and the dark count rate per time window, respectively. In the experiment, η was around 1%, i.e., 20 dB loss, which includes 3 dB coupling loss between fiber pigtails and the waveguide, 7 dB insertion loss of the delay line, filters, and the polarizer, and 10 dB due to the 10% quantum efficiency of the single photon detector. D was around 10^{-6}. The denominator is the coincidence rate away from the HOM dip; the terms inside the denominator are coincidence rates due to single photon pair, multi-photon pair and dark counts, respectively. The numerator is the coincidence rate at the dip, where the single photon pair will not contribute to the coincidence rate due to interference.[1] The terms inside the numerator are coincidence rates due to the multi-photon pair and dark counts. The extinction ratio of the asymetric Y junction was >20 dB for our device making its effect on the visibility negligible.

We set the peak pump power to 4.4 mW by adjusting the variable power attenuator and scanned the fiber delay to observe the HOM dip shown in Fig. 2. From a fit to the data, we estimated the visibility to be $80 \pm 9\%$ and σ as 1.20 ± 0.20 ps, close to the theoretical estimate of 87% and 1.7 ps. Thus, a visibility that indicates quantum interference ($>50\%$) was observed.[2] The backgrounds do not fit very well with the HOM dip curve because of the temperature fluctuation of the waveguides in the experiment, which can be fixed to change a better Peltier effect based temperature controller instead of the oven.

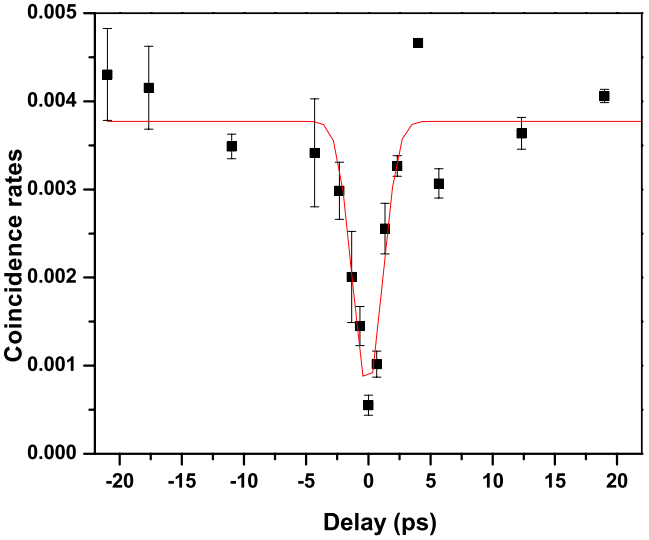

Fig. 2. (Color online) HOM dip. We took three sets of data for each point in the graph to estimate the measurement uncertainty. The error bars result from the data sets' standard deviation.

4. Conclusions

We generated spatially separated frequency-degenerate twin photons and observed the HOM dip using a RPE PPLN waveguide with integrated asymmetric Y-junction mode multi-/demulti-plexer. The HOM dips observed in the experiment originate from quantum interference and are consistent with our theoretical analysis. To increase the brightness of our source, we can reduce the coupling loss between the fiber pigtails and the waveguide with AR coating. We can further reduce the insertion loss of the filters, polarizer and delay line by choosing better products. With lower dark counts and higher bandwidth detector, we can further increase the visibility. Changing the pump laser into CW laser, one can achive near infrared time-energy entanglement source for QOCT instead of visible entanglement.[6] Changing the pump laser into two sequential pulses, one can achieve the time-bin entanglement,[20] which can find applications in LOQC. All previous experiments in LOQC have been implemented using polarization entangled photon pairs. However, a c-not gate[21,22] can be implemented using time-bin entanglement by changing the polarization beam splitter into an optical switch. The use of our waveguide-based source can significantly reduce the footprint of such a setup, compared with sources based on bulk crystals or a few-hundred meters of fiber.[22]

Acknowledgment

This research was supported by NICT, the MURI center for photonic quantum information systems (ARO/ARDA program DAAD19-03-1-0199), SORST, CREST programs, Japan Science and Technology Agency (JST), the U.S. Air Force Office of Scientific Research through contracts F49620-02-1-0240, the Disruptive Technology Office (DTO). We acknowledge the support of Crystal Technology, Inc.

1) C. K. Hong, Z. Y. Ou, and L. Mandel: Phys. Rev. Lett. **59** (1987) 2044.
2) L. Mandel: Rev. Mod. Phys. **71** (1999) S274.
3) D. Bouwmeester, J. W. Pan, K. Mattle, M. Eibl, H. Weinfurter, and A. Zeilinger: Nature **390** (1997) 575.
4) H.-J. Briegel, W. Dr, J. I. Cirac, and P. Zoller: Phys. Rev. Lett. **81** (1998) 5932.
5) E. Knill, R. Laflamme, and G. J. Milburn: Nature **409** (2001) 46.
6) M. B. Nasr, B. E. Saleh, A. V. Sergienko, and M. C. Teich: Phys. Rev. Lett. **91** (2003) 083601.
7) S.-B. Cho and T.-G. Noh: Opt. Express **15** (2007) 7591.
8) J. Chen, J. B. Altepeter, M. Medic, K. F. Lee, B. Gokden, R. Hadfield, S. W. Nam, and P. Kumar: Phys. Rev. Lett. **100** (2008) 133603.
9) M. Halder, A. Beveratos, R. T. Thew, C. Jorel, H. Zbinden, and N. Gisin: New J. Phys. **10** (2008) 023027.
10) H. Takesue: Appl. Phys. Lett. **90** (2007) 204101.
11) J. Fulconis, O. Alibart, J. O'Brien, W. J. Wadsworth, and J. G. Rarity: Phys. Rev. Lett. **99** (2007) 120501.
12) S. Tanzilli, H. De Riedmatten, W. Tittel, H. Zbinden, P. Baldi, M. De Micheli, D. B. Ostrowsky, and N. Gisin: Electron. Lett. **37** (2001) 26.
13) J. Chen, K. F. Lee, and P. Kumar: Phys. Rev. A **76** (2007) 031804(R).
14) J. R. Kurz, J. Huang, X. Xie, T. Saida, and M. M. Fejer: Opt. Lett. **29** (2004) 551.
15) X. Xie and M. M. Fejer: Opt. Lett. **31** (2006) 799.
16) R. P. Tapster and J. G. Rarity: J. Mod. Opt. **45** (1998) 595.
17) H. De Riedmatten, V. Scarani, I. Marcikic, A. Acin, W. Tittel, H. Zbinden, and N. Gisin: J. Mod. Opt. **51** (2004) 1637.
18) H. Takesue and K. Shimizu: Opt. Commun. **283** (2010) 276.
19) Q. Zhang, X. Xie, H. Takesue, S. W. Nam, C. Langrock, M. M. Fejer, and Y. Yamamoto: Opt. Express **15** (2007) 10288.
20) J. Brendel, N. Gisin, W. Tittel, and H. Zbinden: Phys. Rev. Lett. **82** (1999) 2594.
21) T. B. Pittman, B. C. Jacobs, and J. D. Franson: Phys. Rev. A **64** (2001) 062311.
22) A. Politi, M. J. Cryan, J. G. Rarity, S. Yu, and J. L. O'Brien: Science **320** (2008) 646.